Effects of collisionality and T_e/T_i on radiative temperature fluctuations in positive and negative triangularity tokamak plasmas

M. Fontana[1], L. Porte[1], S. Coda[1], O. Sauter[1], S. Brunner[1], Ajay C. J.[1], A. Fasoli[1], G. Merlo[2] and the TCV team‡

[1]Ecole Polytechnique Fédérale de Lausanne (EPFL), Swiss Plasma Center (SPC), CH-1015, Lausanne, Switzerland
[2]University of Texas at Austin, Austin, TX 78712, United States

E-mail: matteo.fontana@epfl.ch

January 2019

Abstract. The effects of negative triangularity (δ) on confinement and fluctuations in plasmas covering a large range of parameters were investigated on the tokamak à configuration variable (TCV). The conditions explored in this paper include discharges where neutral beam (NB) heating was employed to obtain an electron-ion temperature ratio $T_e/T_i \sim 1$ across a large fraction of the plasma profile. This significantly extended the range of negative δ plasmas studied on TCV towards conditions more relevant to future reactor-like tokamaks. Negative triangularity was found to improve confinement over the full range of collisionality studied ($0.1 < 1/\nu_{\text{eff}} < 2$) and T_e/T_i ($0.5 < T_e/T_i < 5$). The amplitude of radiative temperature fluctuations, measured using a correlation electron cyclotron emission (CECE) diagnostic over the range $0.55 < \rho_{\text{vol}} < 0.75$, was found to be reduced, in negative with respect to positive δ plasmas, for all combinations of parameters explored. This was, in particular, verified for a pair of positive and negative δ plasmas with comparable density and q_{95} under different conditions of NB heating. Linear gyrokinetic simulations found the dominant turbulence regime, in the strongly NB heated discharges, to be a mix of trapped electron modes (TEMs) and ion temperature gradient driven modes (ITG). This is in contrast to ohmic or electron cyclotron heated discharges, for which the dominant turbulence regime was found to be pure TEM. Negative triangularity was found to lead to partial stabilization of the most unstable modes for low wavenumbers in both turbulence regimes. These findings demonstrate that negative triangularity could provide significant confinement improvement over a large range of parameters, that include conditions closer to future reactor-like machines ($T_e/T_i \sim 1$, low collisionality).

‡ See author list of S. Coda et al 2017 Nucl. Fusion 57 102011

1. Introduction

Anomalous transport [1] is recognized as the main contribution to heat and particle loss in magnetically confined plasma. It arises from the coupling of microfluctuations of the plasma electric and magnetic fields, with those of the density and temperature profiles. Reducing these fluctuations, which generally develop into a turbulent state, is key to improving confinement and performance in future magnetic confinement machines. Work performed at TCV in the last twenty years has shown that negative triangularity could significantly improve confinement and reduce turbulent fluctuations.

Due to its flexibility, the tokamak à configuration variable (TCV) [2] is particularly useful to investigate the effects of innovative shaping on confinement and fluctuations. TCV is a carbon walled, medium sized tokamak (major radius R = 0.88 m, minor radius a = 0.25 m) with up to 1.53 T magnetic field on axis and up to 1 MA plasma current. One of its important assets is the unparalleled shaping capability that allows the investigation of plasmas with elongation $0.9 < \kappa < 2.8$ and triangularity $-0.7 < \delta < 1$.

In experiments with limited negative δ plasmas, strong confinement improvement was observed for ohmic [3] and EC heated [4, 5, 6, 7] discharges. In particular, similar electron density and temperature profiles were obtained in symmetric positive and negative δ plasmas using only half of the auxiliary heating power in the latter case [5, 6]. The relative confinement improvement between positive and negative δ was found to reduce for increasing collisionality [6], until no beneficial effect of negative δ could be observed in high density, ohmic discharges. Electron density and temperature fluctuation measurements were performed in two different series of L-mode discharges, using the tangential phase contrast imaging (TPCI) [8, 9, 10] and correlation electron cyclotron emission (CECE) [11, 12, 13] diagnostics respectively. Both studies found a marked suppression of fluctuations in negative with respect to positive δ discharges.

The causes of the confinement improvement observed in the experiments were studied using gyrokinetic simulations (LORB5 [14], GS2 [15], GENE [16, 17]). These simulations were performed using the experimental equilibria of positive and negative δ discharges with matched temperature and density profiles. Trapped electron modes (TEMs) were found to be the dominant source of instability in both shapes, for all wavenumbers with $k\rho_s \leq 2$ (where $\rho_s = \frac{\sqrt{T_e/m_i}}{eB/m_e}$) in all studies. TEMs are expected to be stabilized by collisions [18], so these results are consistent with the experimental observation of a reduction of the electron heat conductivity (χ_e) for increasing collisionality [6].

The global, gyro-kinetic, collisionless simulations performed using the LORB5 code, demonstrated reduction of the mixing length heat diffusivity and the growth rate of modes with n<10 in negative δ plasmas. Moreover, the structure of the electrostatic potential fluctuations was observed to change with δ, with higher $k_\perp$ for low n modes, in negative δ discharges [6].

Flux-tube, non-linear simulations, run using the GS2 code, including impurity effects but not collisions, managed to reproduce the reduction of χ_e in negative with respect to positive δ pulses within the experimental error bars, for $\rho_{\text{vol}} = 0.7$, but not for positions closer to the plasma core. There, the χ_e reduction was instead underestimated [19]. Flux-tube GENE simulations based on the same equilibria and profiles, this time including the effects of collisions, again found negative δ to have stabilizing effects only for $\rho \geq 0.7$ but did not reach quantitative agreement with the experimental heat fluxes. These results also suggested that negative triangularity may increase the critical gradient for the onset of turbulent fluctuations [20]. Other gradient-driven, global, non-linear GENE simulations, not including the effects of impurities, qualitatively reproduced the reduction of the heat flux for $\rho > 0.4$, even though their results still exceeded the experimental values [21].

Thanks to these results, interest has grown for the possibility of developing negative δ scenarios for future tokamak reactors [22, 23, 24, 25]. Beside the confinement improvement, in fact, this type of configuration could provide attractive advantages concerning power handling management, which is considered to be one of the major challenges to overcome [26, 27] in designing large tokamaks.

However, the results obtained in past experiments in TCV [4, 5, 6, 9, 10, 13] cannot simply be extrapolated to a reactor-like machine. One of the reasons is that the works cited above only investigated the effects of negative δ on confinement in ohmic or EC-heated discharges, where the electron temperature in the plasma core was more than twice the ion temperature. Instead, in a reactor-like tokamak, it is expected that the confinement time and density will be high enough to allow coupling and thermalization of electrons and ions, leading to $T_e/T_i \sim 1$ across a large fraction of the radial profile. This can have important effects on transport. For example, lower values of T_e/T_i are considered one of the main factors that can drive the change in the turbulence regime from electron to ion dominated.

One other important difference between the discharges used in most of the aforementioned studies and those expected to be used in future reactors is the presence of a divertor. Studies on diverted, upper negative triangularity discharges are, in fact, very

limited. In TCV, L-mode pulses [28] showed a higher edge temperature in negative δ, while in H-mode [7] lower pedestals were found, with respect to symmetric positive δ pulses.

Recently, on DIII-D, L-mode limited discharges with negative triangularity, heated with both ECH and NBI and reaching $T_e/T_i \sim 1$, were obtained. In these discharges, H-mode like confinement without edge pedestal and reduced fluctuations, with respect to positive δ plasmas with the same applied actuators, were observed [29, 30]. Linear gyrokinetic simulations found that the resulting turbulence was dominated by trapped electron modes [29, 30], similarly to what was observed in TCV [19, 20, 21].

TCV has been recently upgraded with a 1 MW neutral beam (NB) heating system [31] that can be used to cover a wide range of previously unattainable operation conditions, especially characterized by $T_e/T_i \lesssim 1$. This possibility was exploited to produce a pair of discharges with symmetrical positive and negative δ, strong ion heating and comparable density and current density profiles. Starting from these model discharges, numerous pulses were obtained, with varying plasma conditions, in order to assemble a database of fluctuation measurements in a large parameter space. The equilibria and experimental profiles of these discharges were used as inputs for linear, flux-tube gyrokinetic simulations, run using the GENE code. The aim of these simulations was twofold. First, it was to understand if these strongly ion-heated plasmas still displayed a purely electron driven turbulence regime or an ITG/TEM mix. Then, to verify if negative δ had stabilizing effects also in the presence of stronger ion gradients and $T_e/T_i \lesssim 1$.

The two closely matched positive and negative δ discharges and the range of conditions explored in the measurements database are described in section 2. The main results obtained from analysis of the measurements on the aforementioned pulses are presented in section 3. In section 4, the details and the main results of the gyrokinetic simulations are reported. Finally, conclusions are drawn in section 5.

2. Experimental method

2.1. Development of matching NBI heated discharges with positive and negative δ

To highlight the effects of triangularity in NB heated plasmas, minimizing the influence of other parameters (such as plasma elongation, safety factor and kinetic profiles), a pair of positive and negative δ discharges as similar as possible were produced. Their geometry is shown in figures 1a and 1b. The two plasmas were centered on the vessel midplane (z=0) and presented symmetric shapes with $\delta = \pm 0.4$, $\kappa = 1.4$. By

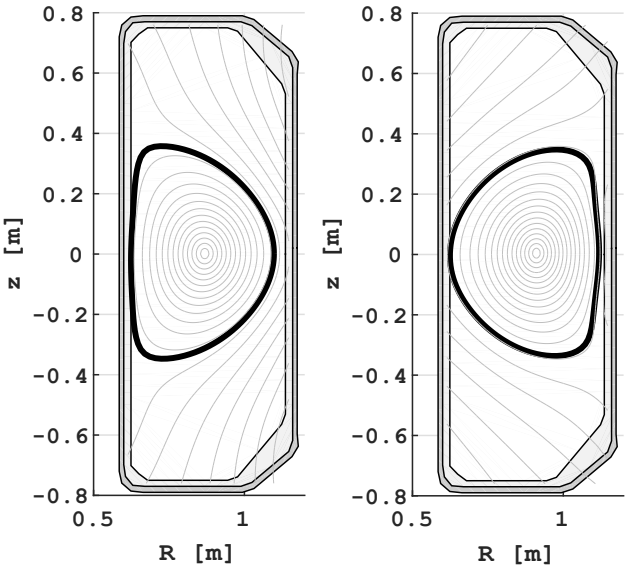

Figure 1: Plasma geometry for the positive (60797) and negative (58499) δ discharges (a and b).

varying I_p in the two differently shaped pulses (265 kA and 230 kA for the positive and negative δ plasmas respectively), comparable safety factors were obtained over the whole radial profile ($q_{95} \sim 3.4$).

It could be argued whether it is I_p or the q profile that mostly influences plasma confinement. In this sense, the choice of a higher I_p for the positive δ plasma is conservative with respect to its possible effect on confinement. Furthermore, negative triangularity had already been found to strongly improve confinement in a pair of positive and negative δ ohmic discharges, with comparable density profiles with the same I_p [13].

Both discharges had central line averaged density $n_{\mathrm{e,av}} = 2.9\ 10^{19}\ \mathrm{m}^{-3}$. This value was calculated after the equilibrium reconstruction, considering the actual intersection of the vertical FIR chord used for the measurement with the plasma volume, in the two different shapes. The negative triangularity discharge was heated with 300 kW of NBI for 1 s, while the positive triangularity one was heated in two different phases, each 0.4 s long, at 300 and 1000 kW respectively. The time traces of the main parameters for the negative and positive δ discharges are shown in figures 2a and 2b respectively. Phases in which the plasma parameters remained stationary were chosen in order to perform correlation analysis. They are highlighted with colours in figures 2a and 2b. Notice that, for the negative triangularity discharge, density was not well controlled and decreases significantly after 1.4 s. In the high power phase of the positive δ discharge, instead, the NBI mulfunctioned at 1.65 s.

The resulting profiles for the time windows highlighted in figures 2a and 2b are shown in figure 3. In the selected phases, the density profiles of the positive and negative δ discharges were comparable.

The ASTRA code [32, 33], together with a dedicated module for NB injection [34], was used to simulate the total beam heating power deposition, the resulting current drive and the effective ohmic power for the two discharges. In TCV it is estimated that $\sim$ 20% of the NBI power is lost in interactions with the beam duct. Of the remaining power injected in these discharges, it was found that a fraction between 8% and 20% escapes the plasma by shine-through or first orbit losses. Finally between 25% and 35% of the fast ions in the plasma undergo charge exchange reactions, escaping confinement before they can transfer their energy to the bulk plasma [35]. This results in 150 kW of absorbed NB power for both discharges when $P_{\mathrm{NBI}} = 300$ kW, and 260 kW when $P_{\mathrm{NBI}} = 1000$ kW in the positive triangularity discharge. Adding the ohmic power, the total heating power was $\sim$ 355 kW for the negative δ discharge, while in the positive δ one was $\sim$ 460 and $\sim$ 470 kW for the low and high power phases respectively. The small difference between the total power for the two different heating phases of the positive δ discharge is related to the increase in plasma temperature which, in turn, causes a reduction of the plasma resistivity. The uncertainties in these estimations were calculated by varying the input of ASTRA and evaluating the dispersion of the results of the simulations. In particular, the electron kinetic profiles were varied by +/-10% and the neutrals density at the last close flux surface was changed between 50% and 200%. The uncertainties estimated in this way were found to be $\sim$25% for the 300 kW phases of both positive and negative discharges and $\sim$50% for the 1000 kW phase of the positive δ pulse. These values are summarized in table 1.

The CECE diagnostic of TCV [12] was used to study radiative temperature fluctuations in these discharges. The horizontal line of sight, located at the vessel midplane (z = 0), was used to optimize the plasma coverage of the diagnostic. The six CECE channels were spaced by 300 MHz, corresponding to $\sim$ 0.5 cm. The diagnostic is estimated to be sensitive to wavenumbers $k_\theta < 0.4$ cm^{-1}[36]. The amplitude of the fluctuations was calculated from cross-correlation analysis, using the techniques described in [13], integrating the cross power spectral density over the 20 - 50 kHz range. This frequency range does not represent the whole bandwidth of turbulent fluctuations. However, these lower frequencies are associated to low k modes, which are expected to be the main contributors to saturated transport levels.

2.2. Construction of a database of fluctuation measurements

Starting from the discharges described above, the parameter space covered in this study was broadened through a series of positive and negative triangularity discharges where density, ECH and NB heating powers were varied.

The database contains 50 limited, L-mode discharges, 32 with positive triangularity ($\delta = +0.4$) and 18 with negative triangularity ($\delta = -0.4$). Elongation varied between 1.4 and 1.5 in both shapes. Plasma current was kept fixed in all discharges at 230 kA, causing differences in the safety factor profiles ($q_{95} \sim 3.3$ and $q_{95} \sim 3.8$ for the negative and positive triangularity discharges respectively). In these plasmas the line averaged density was varied from $1{\cdot}10^{19}$ to $3.5{\cdot}10^{19}$ m^{-3}. EC heating was applied using one or two gyrotrons, pointing slightly off the plasma axis but still inside the q = 1 surface, in order to reduce the impact of sawteeth [37]. Plasmas included in the database, where ECH was applied, were heated using 365 kW, 730 kW or 1000 kW. Neutral beam heating was applied to some of the negative (300 kW) and positive (300 or 1000 kW) triangularity discharges. Taking into account also the ohmic power, the total effective power varied between 150 and 1200 kW in the discharges of the database. In all discharges the plasma axis was set at z = 0 cm in order to have on-axis NB injection when the heating beam was used. The discharges have confinement times varying between 2 and 20 ms.

For all of these discharges, the flat top between 0.5 and 1.5 s was divided into 100 ms intervals. Plasmas were considered stationary in these 100 ms intervals if the plasma density did not vary by more than 15%, and the heating power and mixture did not change. Only such intervals were considered for analysis. Equilibria and current density were also checked to be stationary during the selected intervals.

In all of these discharges, radiative temperature fluctuations were measured with the CECE diagnostic, using settings similar to those of the pair of matched discharges described in section 2.1. For each time interval, fluctuation measurements in five different radial positions were obtained. In some of the discharges, especially positive δ pulses, when high power NBI was applied, quasi-coherent modes could be observed in the 20-25 kHz range in the Cross power spectral density (CPSD). These modes were found to be weaker and rarer in the negative δ plasmas included in this database. To exclude the contribution of these modes from the fluctuation amplitude calculation, they were identified, and their amplitude subtracted with respect to the background spectra around them. For some fluctuation measurements, the optical thickness was too low to guarantee

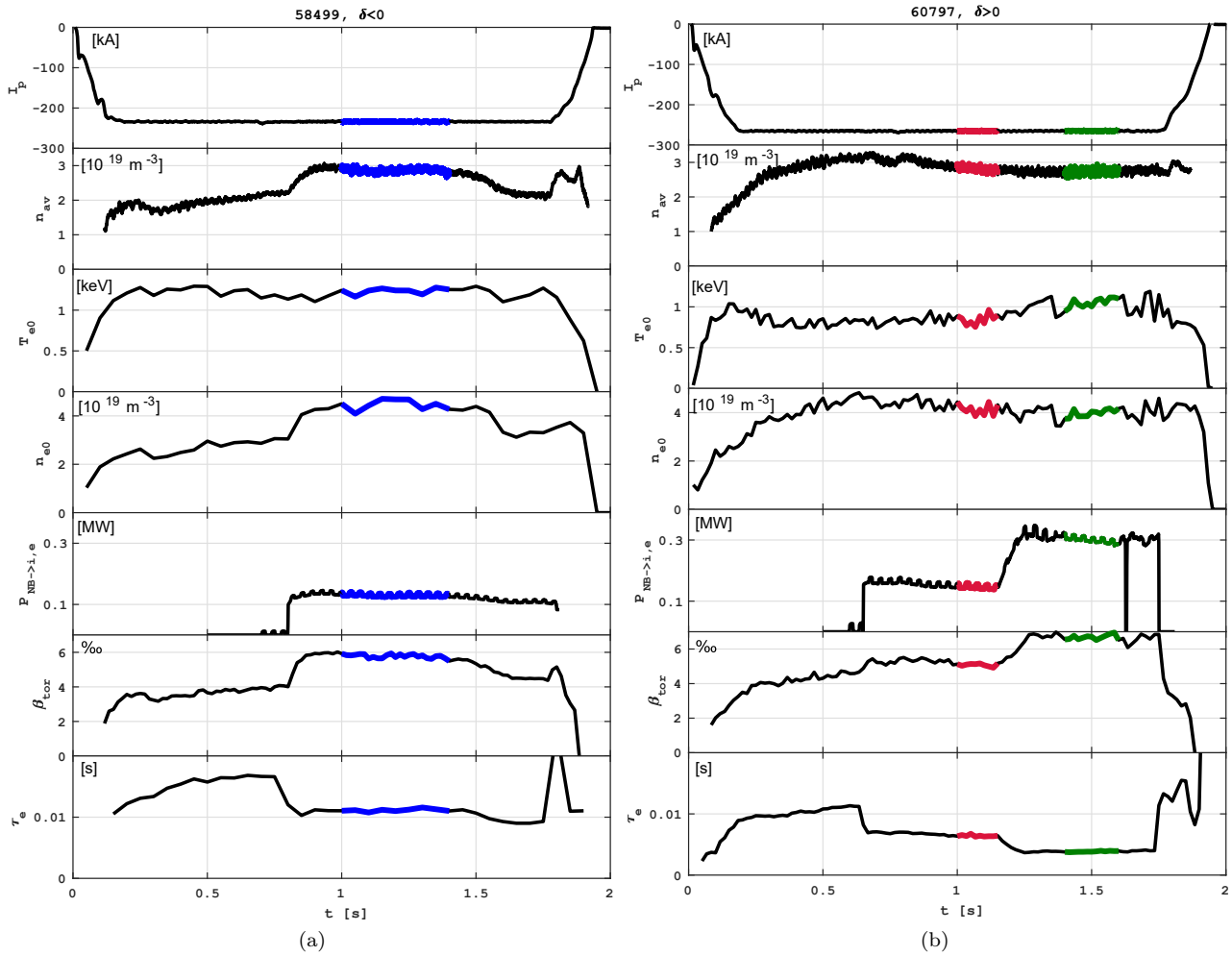

(a) (b)

Figure 2: Time traces for plasma current I_p, line averaged density n_{eav}, core temperature T_{e0} and density n_{e0}, NBI power absorbed by the bulk plasma $P_{\mathrm{NBI->i,e}}$, β_{tor} and energy confinement time τ_E for the reference discharge with $\delta < 0$ (a) and $\delta > 0$ (b). Highlighted are the time intervals over which correlation functions have been computed.

	I_p [kA]	Z_{eff}	P_{NBI} nom. [kW]	P_{NBI} eff. [kW]	P_{ohm} [kW]	P_{tot} [kW]	$H_{98\mathrm{y2}}$	$H_{89\mathrm{P}}$
δ = -0.4	230	2.91	300	150 (25%)	205	355	0.90	0.83
δ = +0.4	265	1.60	300	150 (25%)	310	460	0.55	0.31
δ = +0.4	265	1.60	1000	260 (50%)	210	470	0.65	0.39

Table 1: Summary of plasma current, effective charge, nominal and effective ohmic and auxiliary power injected in the positive and negative δ plasmas described in section 2.1 and the respective confinement enhancement factors $H_{98\mathrm{y2}}$ and $H_{89\mathrm{P}}$. The estimated uncertainties in the beam power deposition are presented in parenthesis.

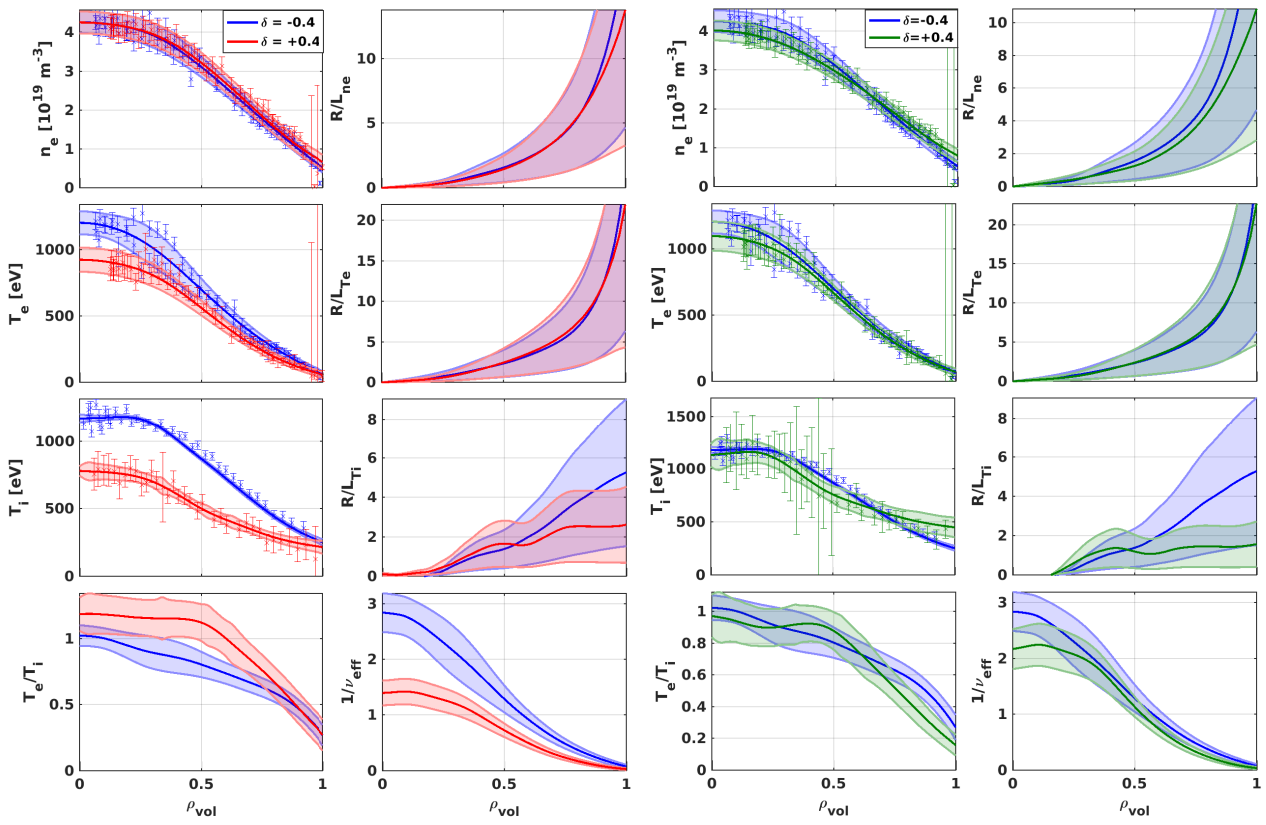

Figure 3: Profiles and normalized scale lenghts for electron density, electron temperature, ion temperature, electron to ion temperature ratio and inverse effective collisionality. The profiles of the negatve δ case (58499), heated with 300 kW (blue), are compared with those of the positive δ case (60797) heated with 300kW (red) and 1000 kW (green).

that the measured radiative temperature fluctuations represented only electron temperature fluctuations. The maximum impact of density fluctuations on radiative temperature fluctuation measurements was conservatively estimated, assuming perfect phasing between density and temperature fluctuations [38, 12], between 3% and 22% depending on the plasma conditions. For the negative and positive δ discharges described in section 2.1, density fluctuations were estimated to account, at most, for $\sim 5\%$ and $\sim 10\%$ respectively. In the following, only fluctuations of the radiative temperature will be discussed.

The database of fluctuation measurements contains a total of 1774 points, of which 1179 in positive δ discharges and 595 in negative δ ones. The local plasma conditions at the measurement points cover the ranges $0.55 < \rho_{\rm vol} < 0.75$, $0.1 < 1/\nu_{\rm eff} < 2$, $0.5 < T_e/T_i < 5$. Here $\nu_{\rm eff}$ is the effective collisionality, defined as the ratio between the electron-ion collision rate and the electron curvature drift frequency. It is approximated as $\nu_{\rm eff} \sim 0.1 R Z_{\rm eff} n_e/T_e^2$ (with T_e in keV, n_e in 10^{19} m^{-3} and R in m) [6, 39]. The measurements of electron temperature and density came from Thomson scattering [40], while $Z_{\rm eff}$ was estimated as constant across the profile. This estimation of $Z_{\rm eff}$ is based on current balance arguments and a neoclassic model [41, 42] that is used to estimate the plasma resistivity, and consequently $Z_{\rm eff}$, consistently with the ohmic current contribution and the measured loop voltage V_{loop}.

The parameter space covered is shown in figure 4 where each point represents the fluctuation measurement of a single pair of channels in one stationary time interval. In that figure the values of $1/\nu_{\rm eff}$, for different values of T_e/T_i (both taken at the measurement points) are plotted versus their radial location. The color of the points is related to plasma triangularity while its hue to the effective total power ($P_{ECH}+P_{NBI}+P_{Ohm}$) applied in the specific discharge and time interval (color online).

This database of measurements was used to in-

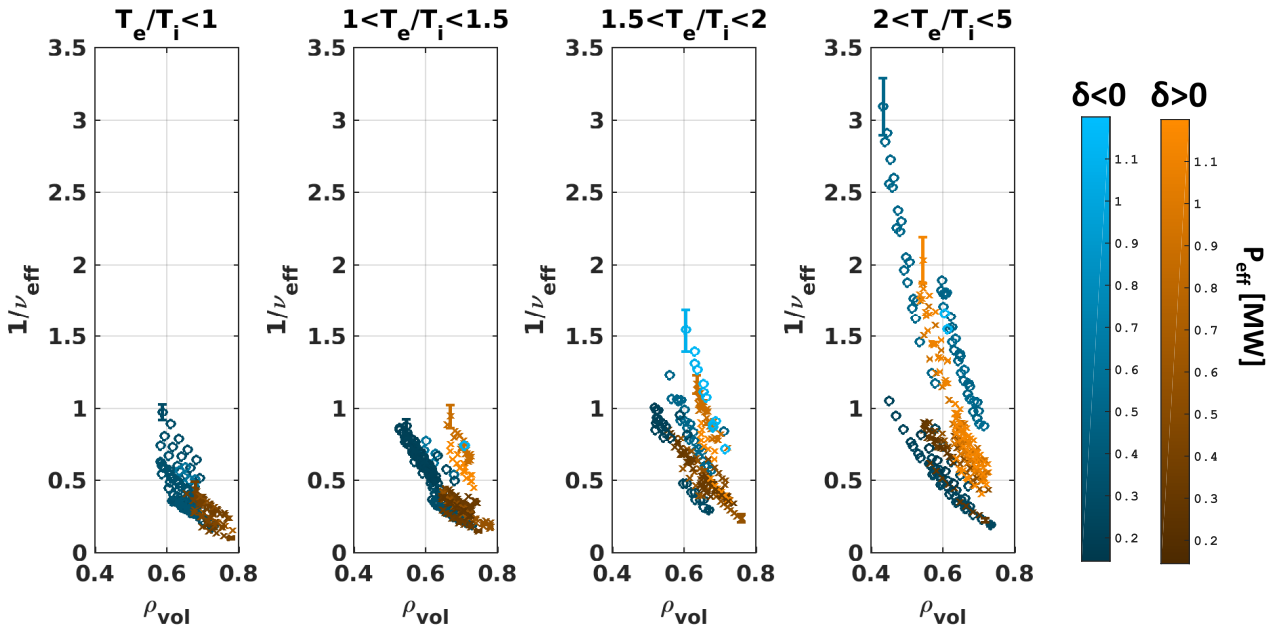

Figure 4: Inverse effective collisionality $1/\nu_{\text{eff}}$ for each fluctuation measurement included in the database, plotted versus the radial location of the measurement. The different subfigures represent different windows of local T_e/T_i. The shade of color is related to the total effective power in the discharge ($P_{\text{ECH}} + P_{\text{NBI}} + P_{\text{Ohm}}$).

vestigate the effects of collisionality and T_e/T_i on fluctuations. Collisionality had already been observed to influence the relative improvement of confinement observed in negative with respect to positive triangularity plasmas [6]. Moreover, collisionality is known to have a stabilizing effect on trapped electron modes (TEMs) [18]. The ratio T_e/T_i, on the other hand, constitutes an important term in determining the relative strength of the ion and electron instability drives.

Another topic of interest was the effect of triangularity on the threshold for the onset of fluctuations [43] and the dependence of the fluctuations amplitude on the normalized temperature gradients [20, 21, 44]. While in this study the local temperature gradient was not tailored by varying the on- and off-axis ECH power within a single discharge [43], the variety of plasma discharges in the database allowed the measurement of temperature fluctuations in pulses with different normalized temperature scale lengths for otherwise very similar plasma conditions. Temperature fluctuation measurements were then used to investigate the effects of triangularity on critical gradients and stiffness.

3. Results

3.1. Confinement and fluctuations in matched positive and negative δ discharges

The left side of figure 3 shows the profiles of the negative δ pulse and those of the low power phase of the positive δ pulse (both heated with $P_{NBI} = 300$ kW). Even though the positive δ plasma is subjected to ∼100 kW more of effective heating than the negative δ one (∼460 kW versus ∼355 kW, see table 1), the latter still presents higher electron and ion temperatures across the whole profile, as was observed for ohmic plasmas [13]. In both cases, ion heating successfully increases the ion temperature to a point where $T_e/T_i \sim 1$ across a large part of the radial profile, in contrast to previous experiments in TCV [4, 5, 6, 9, 10, 11, 13].

In the high power phase of the positive δ plasma ($P_{NBI} = 1000$ kW), whose profiles are shown in the right side of figure 3, the electron and ion temperature profiles are almost matched with that of the negative δ plasma. This is despite the fact that the negative δ plasma is effectively subjected to ∼70% effective heating power with respect to the high power positive δ case.

The heat conductivity for ions and electrons in the three phases discussed in section 2.1 is shown in figure 5. There, ion heat conductivity (χ_i) is substantially higher in positive with respect to negative triangularity, for both NBI heating phases. The difference between the two shapes is observed all the way up to the plasma midradius, similarly to what was observed in previous works [6].

The confinement enhancement for these discharges was calculated as the ratio between the measured confinement time and the confinement time calculated using the $ITER_{H98P(y,2)}$ and the $ITER_{89-P}$ scaling

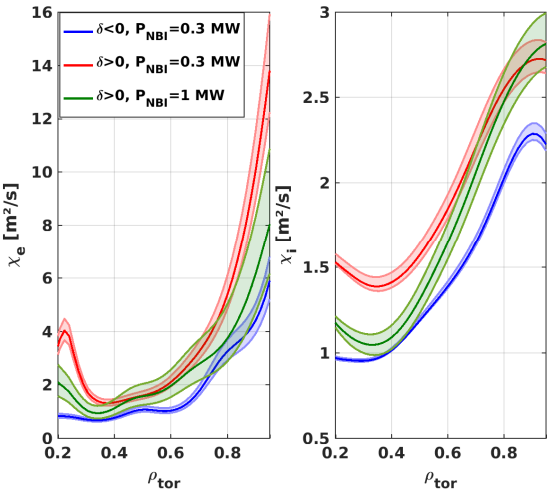

Figure 5: Electron and ion heat conductivity for the three phases of positive and negative triangularity discharges described in section 2.1.

laws [45, 46], obtaining 0.9, 0.55 and 0.65 and 0.83, 0.31, 0.39, in the two scalings, for the negative δ plasma and the low and high power phases of the positive δ one respectively. These values are also reported in table 1. These observations are very important, since they show that negative triangularity could maintain its beneficial effect on confinement also in plasmas closer to those expected in a reactor-like machine, where ions and electrons are thermalized.

Radiative temperature fluctuations were measured, for these plasmas, in the region $0.57 < \rho_{vol} < 0.78$, and the corresponding amplitudes are shown in figure 6. The fluctuations in the negative δ plasma are extremely close to the noise level, while those in the positive δ plasma are well above it. The difference is clear both in the relative and the absolute fluctuation amplitude (figures 6a and 6b respectively). This is similar to what was observed in positive and negative δ ohmic discharges when the same horizontal line of sight was used [36].

Besides injecting energy, the NBI is also a strong source of momentum that drives plasma rotation. The tangential NBI available to TCV, when used on axis, mainly induces strong toroidal rotation. This can be seen in figure 7a, where the toroidal angular velocity (Ω_{tor}) profiles of the positive and negative δ plasmas are shown.

Due to the toroidal momentum, the measured CECE spectra could, in principle, not reflect the actual turbulence spectra. On one side this can be due to the fact that the spectrum becomes dominated by Doppler broadening. On the other hand, increased toroidal velocity and changes to the pressure profile, could have a suppressing effect on fluctuations through an increase of the ExB shear (ω_{ExB}). The observed reduction of fluctuation amplitude, then, could be due not to a change in the turbulence characteristics of the plasma, but to one, or both, of these effects. The ExB shear in these discharges was estimated as [47, 48]:

$$\omega_{ExB} = \frac{r}{q}\frac{d}{dr}\left[\frac{q}{r}\frac{E_r}{B}\right], \tag{1}$$

where r is the distance from the magnetic axis, q the local safety factor, and E_r the radial electric field. The latter was calculated, for the carbon ions, as:

$$E_r = \frac{1}{Z_C n_C}\frac{\partial p_C}{\partial r} - R\Omega_{tor}B_\theta, \tag{2}$$

where B_θ is the poloidal magnetic field, Z_C is the charge state of carbon ions ($Z_C = 6$) and p_C is their pressure. By decomposing the E_r in its diamagnetic and rotational components, it was possible to estimate the relative impact of the two terms, and evaluate their relative impact on ω_{ExB}. They are shown in figure 7b with dashed (diamagnetic) and full (rotational) lines. As expected in L-mode plasmas with NB heating, the rotational component is always larger than the diamagnetic one. The confinement improvement observed in negative triangularity does not appear to increase the diamagnetic contribution. At the same time, increased rotational contribution to ω_{ExB} can be observed in the negative triangularity case with respect to the two positive triangularity ones, for the radial position where fluctuations were measured ($0.57 < \rho_{vol} < 0.78$). However it is important to stress that these estimations are characterized by large uncertainties ($\sigma_{\omega_{ExB}}/\omega_{ExB} \sim 0.5$), so no clear conclusions could be drawn from these results.

These experiments showed that, also in discharges where $T_e/T_i \sim 1$ across most of the radial profile, and thus closer to reactor relevant regimes, negative triangularity has beneficial effects on confinement and suppresses fluctuations. In particular, the reduction in fluctuation amplitude measured with the CECE is consistent with recent observations on DIII-D, where the same technique was applied to L-mode, limited positive and negative δ plasmas heated with both EC and NB [30, 29]. It is important to highlight that other factors that might have influenced the final transport levels, such as the safety factor profile and elongation, were remarkably similar in the two discharges discussed here. In these experiments, however, it was not possible to decouple ion heating from the injection of toroidal momentum which could have a significant effect on the resulting turbulence.

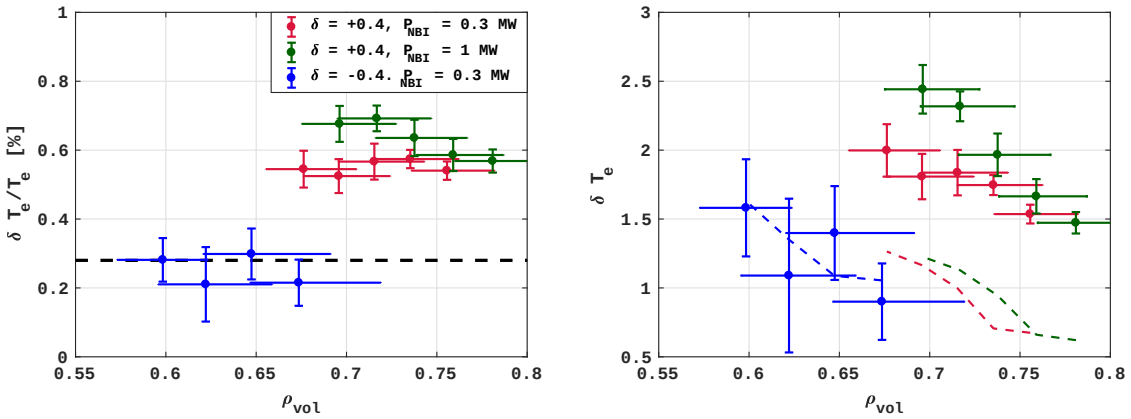

(a) (b)

Figure 6: Relative (a) and absolute (b) amplitude of the fluctuations obtained by integrating the CPSD of neighbouring channels between 25 and 50 kHz. Dashed lines represent the estimated noise levels for the measurements.

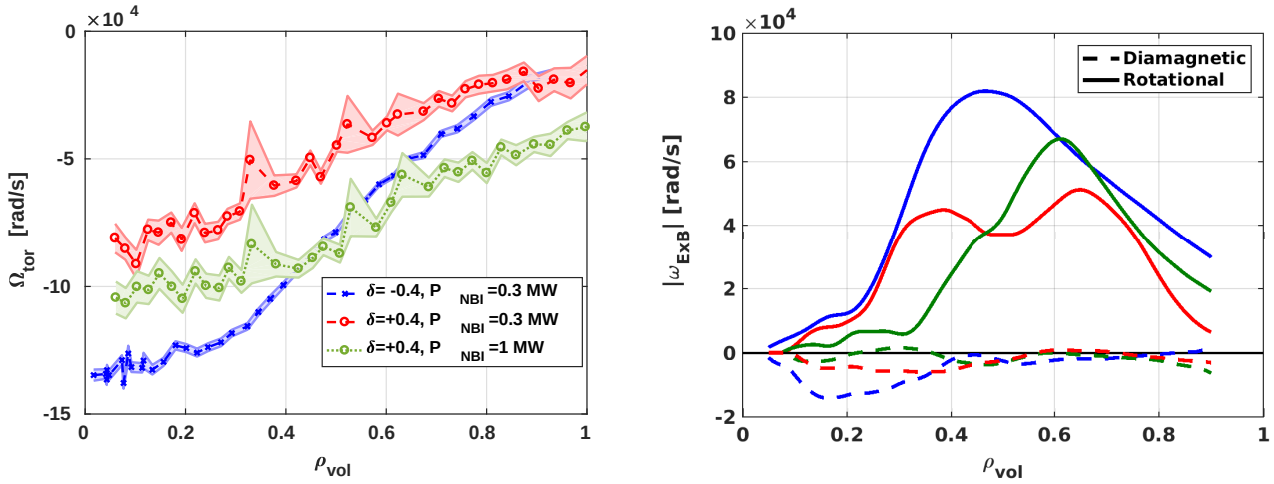

Figure 7: (a) Toroidal angular speed of the carbon ions in the plasma as measured by the CXRS); (b) estimated diamagnetic and rotational components of ω_{ExB} in the NBI heated discharges presented in this paper

3.2. Confinement improvement over a large parameter space

Similar analyses were carried out on all the discharges described in section 2.2.

For the pulses in this group in which NBI was applied, the confinement time was compared with that predicted by the $ITER_{89-P}$ scaling law [46], calculated taking into account the effective NBI power transferred to the plasma. Figure 8 shows the confinement enhancement factor as a function of the inverse volume averaged effective collisionality $1/ < \nu_{\rm eff} >$ [6, 39] and T_e/T_i at the plasma core. In this figure each point represents the plasma conditions in a stationary time interval for one of the database discharges. Negative triangularity discharges are found to generally present better confinement with respect to positive triangularity ones, for similar plasma conditions. Most interestingly, this includes plasmas with high collisionality and low T_e/T_i, conditions that could not be achieved on TCV before the installation of the NBI. This database, though, does not contain discharges with sufficiently high $\nu_{\rm eff}$ to probe the part of the parameter space where the relative confinement improvement in negative compared to positive δ discharges was found to be strongly reduced [6] ($\nu_{{\rm eff},\rho=0.55} \sim 2$, $1/\nu_{{\rm eff},\rho=0.55} \sim 0.5$). It is important to stress, however, that inductive plasmas in ITER are designed to have $\nu_{eff,\rho=0.55} \sim 0.25$ or $\nu_{eff,\rho=0.55} \sim$

0.05 in L-mode and H-mode respectively [49], well inside the range where negative δ has the strongest effects.

3.3. Effect of collisionality on fluctuations

The fluctuation measurements composing the database have been plotted against the corresponding $1/\nu_{\text{eff}}$ in figure 9, for all time intervals and discharges. Notice that ν_{eff} in this case is the local value of collisionality at the measurement position while, in figure 8, only the volume averaged value was considered.

For all ν_{eff} values, at comparable radial positions, fluctuations are higher in positive δ than in negative δ plasmas. In both shapes, fluctuation amplitude decreases with increasing collisionality, with the difference between positive and negative triangularity reducing strongly for high ν_{eff} values. This result is consistent with previous observations for density fluctuations [9, 10] and with past calculations of electron heat conductivity [6]. It is important to notice that all fluctuation amplitudes below the diagnostic sensitivity level (represented by the solid black line in the plot) are characterized by relatively large uncertainties and represent measurements in which very little meaningful fluctuation was detected.

It is particularly interesting that also for plasmas where $T_e/T_i \leq 1$, obtained using NBI heating, fluctuations are higher in positive δ cases for a large range of collisionalities. This is highlighted in figure 10, where only measurements made in plasmas for which $(T_e/T_i)_{\rho=0} \leq 1.1$ are shown. This is consistent with what has already been discussed in section 3.1 and is promising for the potential of a reactor-like tokamak with negative δ.

The separate effect of effective charge on the measured fluctuation amplitude, for comparable collisionality, was also investigated. A strong fluctuation reduction in negative triangularity plasmas was still found for similar values of Z_{eff} and comparable collisionality, suggesting the effect of impurities is weak compared to that of shaping in these cases. This is shown in figure 11, where the same data of figure 9, limited to $0.6 < \rho < 0.65$, is plotted as a function of Z_{eff}.

3.4. Effect of T_e/T_i on fluctuations

Measurements assembled in this database also allowed to observe the effects on the fluctuation amplitudes of varying T_e/T_i, an important factor for determining the drive of different turbulent modes. In figure 12 the same set of data as in figure 9 (limited to $0.65 < \rho_{vol} < 0.7$) is plotted directly against T_e/T_i. While a positive correlation between $\delta T_e/T_e$ and T_e/T_i could be deduced by some of the plots in figure 12, the dependence is found to be mainly related to T_e alone. This latter dependence is to be expected due to the dependence of fluctuation amplitude on ν_{eff} illustrated in figure 9 and the fact that $\nu_{\text{eff}} \propto 1/T_e^2$. If that is taken into account, the temperature ratio does not seem to have a direct effect on fluctuations for the parameter space studied in this database. No clear trend can be identified.

Suppression of fluctuations in negative δ plasmas can still be observed across the whole range of T_e/T_i explored. Only in a few cases do the measurements in positive and negative δ show comparable levels of fluctuations for similar T_e/T_i. It is not excluded that T_e/T_i could influence plasma fluctuations and the relative confinement improvement in negative with respect to positive triangularity pulses. The fact that no direct effect of T_e/T_i can be recognized may, in fact, be due to the limited range of plasma parameters covered by this database (*e. g.* too small range of density), or to the limited sensitivity of the diagnostic to small fluctuating structures.

3.5. Effect of pressure gradients on fluctuations

As already mentioned, it was suggested that negative triangularity could act on the gradient threshold necessary for the onset of turbulent modes [20]. To evaluate this effect, the fluctuation amplitudes shown in figure 12 are plotted in figure 13, as a function of the local normalized electron temperature scale length ($\frac{R}{L_{T_e}} = \frac{R}{\nabla T_e/T_e}$). There, it is possible to observe how fluctuations in negative δ discharges are, in almost all cases, lower than in positive δ ones for comparable normalized gradients. In the first two subfigures, in particular, the trend of increasing fluctuation amplitude with increasing drive is visible for both plasma shapes. This suggests that negative triangularity could increase the gradient threshold for the onset of turbulence, decrease the sensitivity of fluctuation amplitude on the driving gradient, or a combination of both these effects. This explanation is similar to that proposed for the effects of triangularity on the onset of turbulent heat flux [20]. To properly test these hypotheses, though, dedicated experiments with varying amounts of ECH power deposited inside and outside the measurement location would be necessary. This is however outside the scope of this paper [43].

The depedence of fluctuations on R/L_{ne}, also an important drive for TEMs, is shown in figure 14. It was observed that, for higher values of collisionality, R/L_{ne} reduced the measured fluctuation amplitude, for both positive and negative δ plasmas. This is an unexpected observation since a larger turbulence drive should correspond to increased fluctuations. Comparing these observations with those in figure 13, it can be argued that, in these cases, R/L_{Te} is the

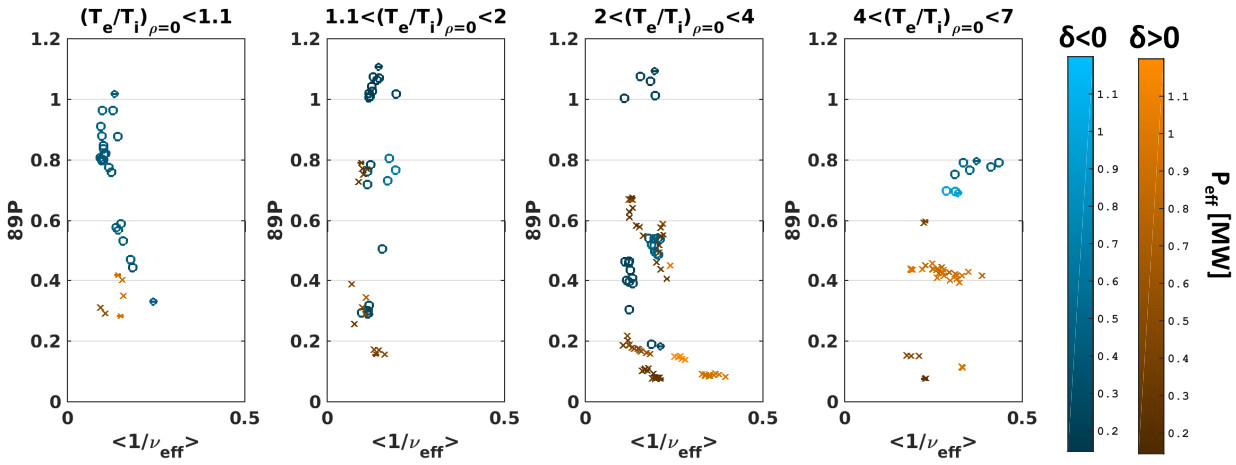

Figure 8: Confinement enhancement factor H_{89P} for each time interval and discharge considered in the database. The data are divided in windows according to the electron-ion temperature ratio at the plasma core. The shade of color is related to the total effective power in the discharge ($P_{ECH} + P_{NBI} + P_{Ohm}$).

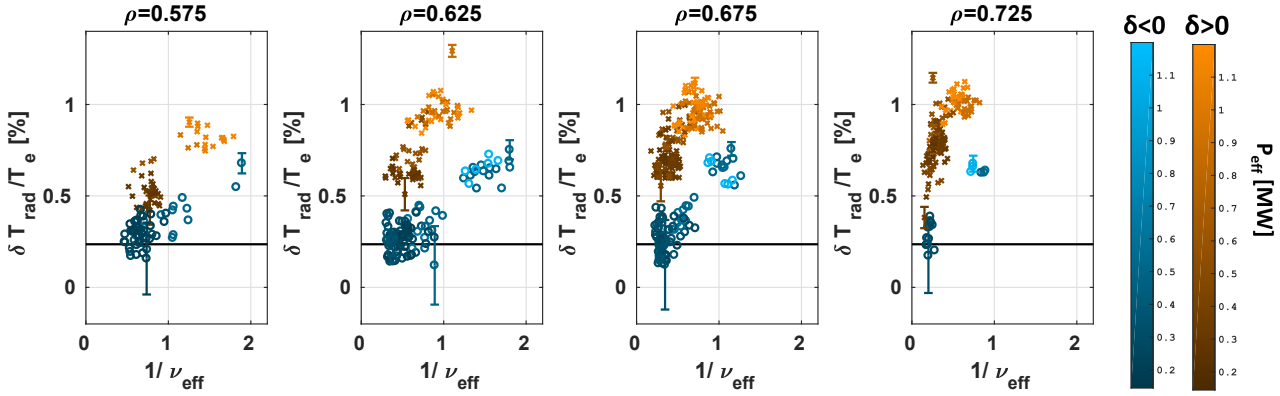

Figure 9: Relative T_e fluctuations (in %) in positive and negative triangularity as a function of $1/\nu_{\text{eff}}$ for various radial positions ($\Delta\rho = 0.05$). The black lines represent the estimated sensitivity limit for fluctuation detection, below which fluctuations are indistiguishable from noise.

dominating drive, as a much clearer effect can be seen for the same conditions. No clear relation was instead found between the measured fluctuations and R/L_{Ti} (not shown), suggesting that, for the largest part of the explored parameters space, turbulence in these plasmas was TEM.

4. Linear GENE simulations

In order to explain the observed effects of triangularity on fluctuations, a comparison with turbulence models is necessary. This would in principle require one to carry out nonlinear (potentially global) simulations trying to reproduce the transport and flucutations levels. Such an exercise is particularly long and expensive and remained outside the scope of this paper. Here only the results of linear, flux tube simulations are discussed, with the aim of comparing the effects of negative triangularity in ohmic and NB heated plasmas. The main goal was to determine the dominant turbulence regime for discharges with comparable electron and ion heating, reaching low T_e/T_i, such as those presented in section 2.1, and verify if gyrokinetic simulations found negative δ to have a stabilizing effect also in these cases.

4.1. Methods

A series of linear, flux-tube gyrokinetic simulations was run using the Eulerian code GENE. Details about the code, together with the definition of the main quantities used in this section, can be found in [16][17]. In these simulations, the input equilibria and pressure profiles were derived from experimental measurements

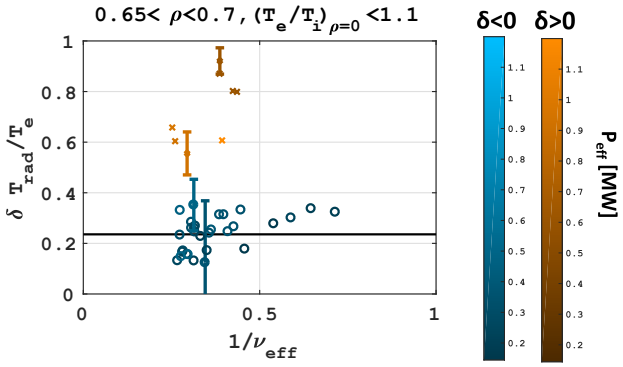

Figure 10: Relative T_e fluctuations (in %) in positive and negative triangularity as a function of $1/\nu_{\text{eff}}$ for $0.65 < \rho < 0.7$. Only points corresponding to discharges for which $T_e/T_i \leq 1.1$ at the core are plotted.

taken in two different pairs of positive and negative δ discharges: one NBI heated and one ohmic pair, with much lower ion drives.

The discharges discussed in section 2.1 constituted the reference pair of NBI heated plasmas whose profiles and equilibria were used in the simulations.

A pair of ohmic discharges with symmetric equilibria, comparable density and similar safety factor profiles was developed. Their main parameters were: plasma current I_p =215 kA ($\delta < 0$) and I_p =235 kA ($\delta > 0$), line averaged density $n_{\text{e,av}}$ =1.9×10^{19} m^{-3}, elongation $\kappa = 1.4$ and $\delta_{95} = -0.4$ and $+0.4$. The two plasmas presented comparable density profiles, while the electron temperature in the negative δ discharge was ∼1.3 times that in the positive δ discharge, despite the total ohmic power being ∼210 and ∼290 kW for the negative and positive δ discharges respectively.

For all discharges, the electron temperature and density profiles were fitted starting from the measurements collected by the Thomson scattering diagnostic [40]. The density and temperature profiles of carbon, considered to be the main impurity in TCV, were obtained by fitting the measurements of the CXRS [50], and the same temperature profile was assumed for carbon and deuterium. The density profile of deuterium was determined imposing charge neutrality, considering carbon to be the only impurity.

For each of the two pairs of discharges, a first set of simulations was run using as input both the magnetic equilibrium and the profiles of the negative δ discharge. A second set used instead the magnetic equilibrium of the positive δ plasma, keeping the remaining parameters unchanged. Each set of simulations consisted in the calculation of the frequency and growth rates for the most unstable modes at different wavenumbers and for different radial positions. The wavenumber scan covered $0.2 < k_y\rho_s < 2$.

The simulations included the effects of collisions and electromagnetic effects, and considered three fully kinetic species: deuterium and carbon ions, and electrons. A summary of the input parameters for the simulations in the different cases is shown in tables 2.

Keeping the kinetic profiles constant and swapping the positive and negative δ equilibria [19, 20] clearly highlights the effects of triangularity, but it is not ideal. It can, in fact, hide the effects that varying triangularity has on other plasma parameters, which, in turn, influence the unstable modes. On the other side, using the experimental profiles as inputs for the simulations would require an analysis of the sensitivity of the simulations to the uncertainties in the inputs, which is outside the scope of this work. A discussion of non-linear gyrokinetic simulations results, using the experimental profiles for the plasmas described in section 2.1, can be found in another work [51].

4.2. Results

The results of the simulations on the ohmic discharges are displayed in figure 15 where the linear growth rate γ and frequency ω of the most unstable mode are shown for wavenumbers $k_y\rho_s < 2$. All quantities are represented in physical units. At all three radii, unstable modes are observed to propagate almost exclusively in the electron diamagnetic direction ($\omega < 0$, also highlighted with full markers in the graphs) allowing their identification as TEM for low $k_y\rho_s < 1$. This situation is very similar to what was observed in past works for gyrokinetic simulations run using the profiles of EC heated positive and negative triangularity plasmas. In fact, also in those cases, the unstable modes were found to be TEM dominated for all wavenumbers [19, 21].

In simulations run with negative δ equilibria, the linear growth rate for the most unstable mode is found to be smaller than in simulations where the positive δ equilibrium was used. This effect is observed particularly for low wavenumbers ($k_y\rho_s < 1$) and for radial positions closer to the plasma edge, where, for selected wavenumbers, γ is up to 50% lower in the negative triangularity case.

The results for the NBI heated discharges are shown in similar plots in figure 16. The main difference in inputs between these simulations and the one performed using the profiles of ohmic discharges is $T_e/T_i < 1$ (see table 2). Also in these simulations, negative triangularity was found to have a stabilizing effect on the most unstable modes at low wavenumbers ($k_y\rho_s < 1$).

At all radial positions, some of these modes show positive frequencies, which, normally, would

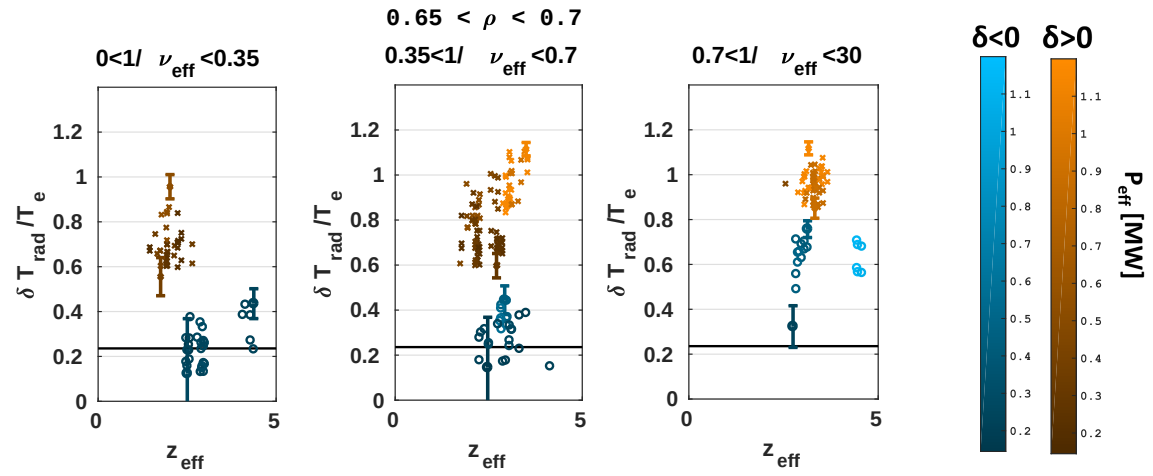

Figure 11: Relative T_e fluctuations (in %) in positive and negative triangularity as a function of Z_{eff} for $0.65 < \rho < 0.7$ and $1/\nu_{\text{eff}}$. All the points in these plots correspond to points shown in figure 9.

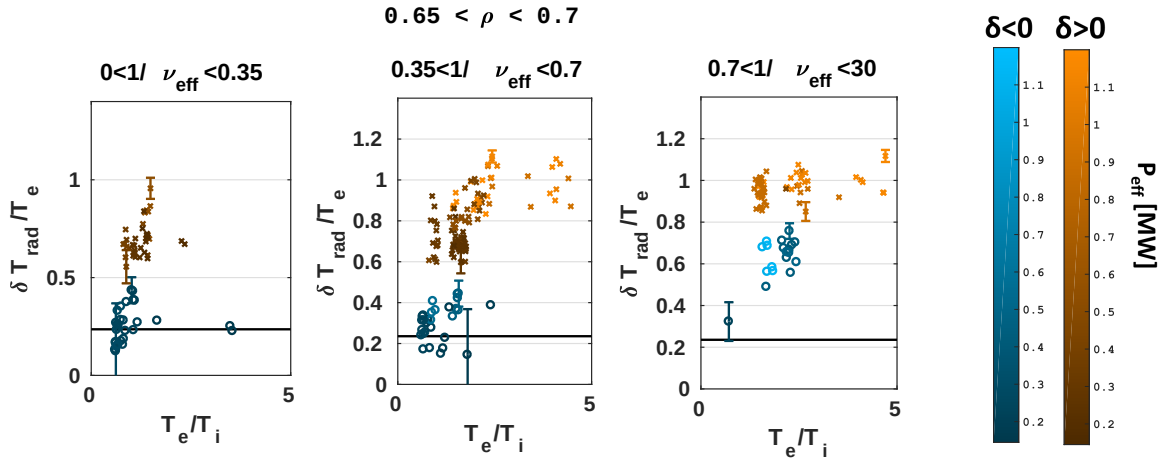

Figure 12: Relative T_e fluctuations (in %) in positive and negative triangularity as a function of T_e/T_i for different combinations of radial positions ($\Delta\rho = 0.05$) and $1/\nu_{\text{eff}}$. All the points in these plots correspond to points shown in figure 9.

be associated to ITG. In these cases, though, the identification of the nature of these modes is complicated by the fact that the quasilinear fluxes resulting from the simulations show the electron contribution to be dominant. Non linear simulations are necessary to fully understand the nature of these modes. The only exceptions are the modes found for low wavenumber at $\rho_{tor} = 0.8$ for positive triangularity, which can be unambiguously identified as ITGs. Interestingly, negative triangularity retains a stabilizing effect on growth rates also in these cases.

Besides the variation in the linear growth rate of the most unstable modes, another way in which triangularity could affect the saturated turbulence regime is through changes in the $E \times B$ shearing rate ($\omega_{E\times B}$). As already mentioned in section 3.1, $\omega_{E\times B}$ contributes to the suppression of turbulent eddies [52]. The $E \times B$ shearing rates associated to toroidal flows were estimated with the definition used by GENE:

$$\omega_{E\times B} = -\frac{\rho_{tor}}{q}\frac{\partial \Omega_{tor}}{\partial \rho_{tor}}, \tag{3}$$

where q is the safety factor and Ω_{tor} is the toroidal angular velocity. The latter is calculated dividing the toroidal velocity, measured by the CXRS [50], by the radial positions of the measurement points. The toroidal angular velocity was considered to be a flux surface quantity. The calculated values of $\omega_{E\times B}$ are shown as solid horizontal lines, in the γ plots of figures 15 and 16, for the ohmic and NBI heated discharges respectively.

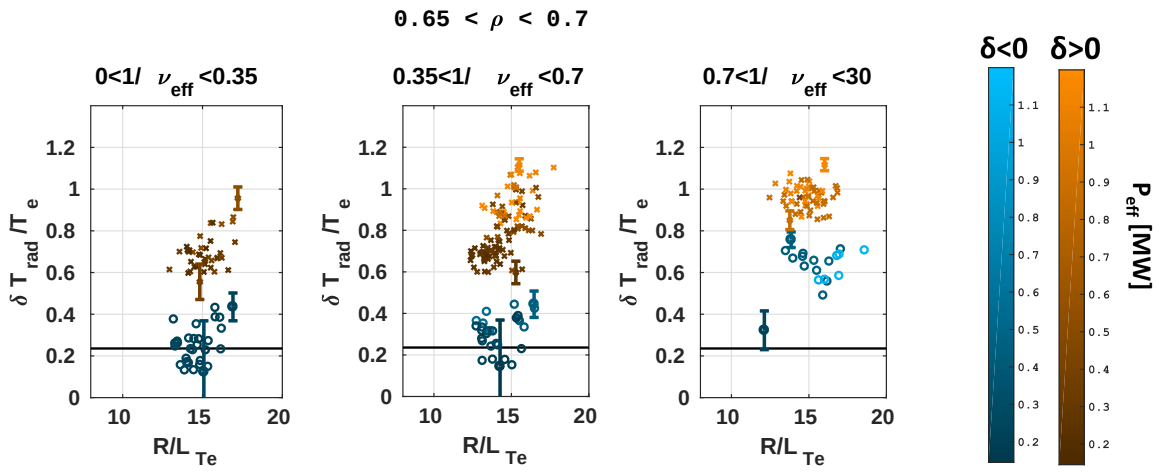

Figure 13: Relative T_e fluctuations (in %) in positive and negative triangularity as a function of R/L_{T_e} for all radial positions. All the points in these plots correspond to points shown in figure 9.

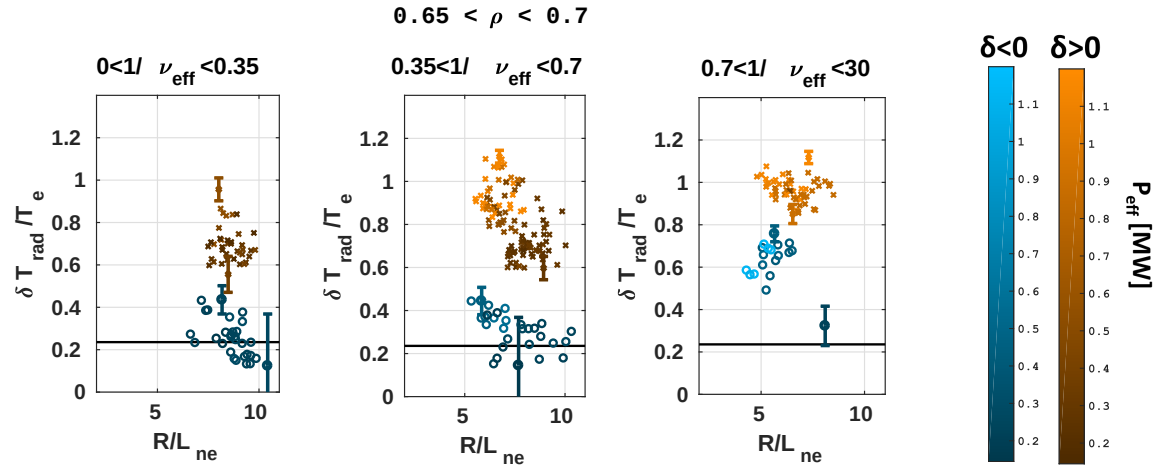

Figure 14: Relative T_e fluctuations (in %) in positive and negative triangularity as a function of R/L_{n_e} for all radial positions. All the points in these plots correspond to points shown in figure 9.

In the ohmic cases, the estimated $\Omega_{E\times B}$ is low with respect to the linear growth rate of the most unstable modes and is thus expected not to strongly affect microinstabilities. In the NBI discharges, instead, the two frequencies are found to be of comparable magnitude. This suggests that the $E \times B$ shearing rate could play an important role in the final saturated state of the turbulence when NB heating is applied. To properly investigate these effects, though, a series of non linear simulations is necessary.

While for both sets of discharges a small difference can be observed in $\omega_{E\times B}$ between positive and negative δ at comparable radii, this is too small with respect to the estimated uncertainties ($\sigma_{\omega_{E\times B}}/\omega_{E\times B} \sim 0.5$) to be uniquely attributed to an effect of shaping.

Linear simulations were also used to investigate the effect of negative triangularity on the threshold gradient necessary for destabilizing modes. Starting from the equilibria and profiles of the NB heated discharges described above, for $k_y\rho_s = 0.4$, R/L_{T_e} was lowered until no mode was excited. As it is shown in figure 17, modes become stable in negative trinagularity at higher R/L_{T-e} with respect to positive triangularity. This is qualitatively consistent with the results of previous non-linear simulations [20] and with the database of measurements showed in figure 13. The positive γ observed for $R/L_{T_e} \sim 0$ is due to the finite value of R/L_{n_e}.

In conclusion, these simulations show that negative triangularity influences the microinstabilities that are driven in tokamak plasmas, resulting in more stable modes. The effect is strongest for low wavenumbers, which are normally associated with larger contributions to overall particle and

ρ_{tor} =0.55										
	q	$\hat{s}$	δ	a/R	T_e/T_i	R/L_n	R/L_{T_e}	R/L_{T_i}	$\nu_{ei} \cdot c_s/R$	β
Ohmic, $\delta > 0$	1.43	1.05	0.14	0.344	1.43	4.48	10.85	5.78	0.56	0.0027
Ohmic, $\delta < 0$	1.32	1.03	-0.15	0.324	1.43	4.48	10.85	5.78	0.56	0.0027
NBI, $\delta > 0$	1.26	1.04	0.13	0.338	0.76	6.16	6.87	5.49	0.73	0.0033
NBI, $\delta < 0$	1.39	0.93	-0.13	0.326	0.76	6.38	7.12	5.69	0.74	0.0036

ρ_{tor} =0.685										
	q	$\hat{s}$	δ	a/R	T_e/T_i	R/L_n	R/L_{T_e}	R/L_{T_i}	$\nu_{ei} \cdot c_s/R$	β
Ohmic, $\delta > 0$	1.90	1.61	0.20	0.344	1.15	5.27	11.54	7.25	1.13	0.0013
Ohmic, $\delta < 0$	1.74	1.51	-0.21	0.324	1.15	5.27	11.54	7.25	1.13	0.0013
NBI, $\delta > 0$	1.67	2.23	0.18	0.338	0.49	10.69	13.82	6.17	1.58	0.0013
NBI, $\delta < 0$	1.79	1.39	-0.18	0.326	0.56	11.08	14.32	6.39	1.64	0.0014

ρ_{tor} =0.8										
	q	$\hat{s}$	δ	a/R	T_e/T_i	R/L_n	R/L_{T_e}	R/L_{T_i}	$\nu_{ei} \cdot c_s/R$	β
Ohmic, $\delta > 0$	2.57	2.32	0.27	0.344	1.00	9.36	12.24	6.69	3.35	0.0004
Ohmic, $\delta < 0$	2.28	1.98	-0.29	0.324	1.00	9.36	12.24	6.69	3.35	0.0004
NBI, $\delta > 0$	2.26	2.23	0.25	0.338	0.49	3.84	8.14	5.96	2.43	0.0007
NBI, $\delta < 0$	2.29	1.85	-0.24	0.326	0.49	3.97	8.44	6.18	2.46	0.0007

Table 2: Parameters used in the GENE simulations for the different shapes, plasma conditions and radial position. The quantities are defined in the main text.

heat transport. The results of these simulations are consistent with the experimental observations discussed in section 3.1 and a series of past works [11, 9, 13]. In particular, this effect was observed not to be limited just to mainly electron driven discharges, where $T_e/T_i > 1$ as in the past [19, 20]. The same effect was observed also when using profiles and equilibria of discharges with comparable electron and ion heating, higher ion gradients and $T_e/T_i < 1$. This is closer to what is expected to happen in future, larger machines. The increased toroidal rotation observed in the NB heated discharges is found to potentially generate a high enough $\omega_{E\times B}$ to influence the saturated state of turbulence, but no clear evidence of an effect of δ on $\omega_{E\times B}$ could be observed. These effects should be the subject of further studies, including both experiments and non-linear gyrokinetic simulations, in order to fully understand their relevance in turbulence suppression.

5. Conclusions

The effects of negative triangularity on confinement and electron temperature fluctuations were studied in plasmas covering a large parameter space in collisionality and T_e/T_i. This work included ion heated discharges, previously not explored in TCV.

Confinement was found to be improved and fluctuations reduced in negative triangularity plasmas, for all combinations of explored parameters. This held true also at low collisionality and low T_e/T_i, a situation closer to those expected in a reactor-like tokamak. In particular two NB heated discharges with symmetric shapes and comparable pressure profiles were obtained applying ~ 0.7 times the total heating power in the negative δ case (355 kW) with respect to the positive δ one (470 kW).

Collisionality was observed to have a suppressing effect on fluctuations, with smaller differences between fluctuations in positive and negative δ found for increasing $\nu_{\rm eff}$, consistently with past observations [6, 9, 10]. It is important to highlight that the range of collisionality and T_e/T_i predicted for ITER [49] is fully inside the parameter space where negative triangularity was observed to have strong effects.

Fluctuations in negative δ discharges were also found to be of lower amplitude than in positive δ ones, for similar temperature and density scale lengths ($R/L_{\rm Te}$, $R/L_{\rm ne}$), at the same radial position and for comparable plasma conditions. This supports the argument that negative triangularity affects the onset mechanism of fluctuations, increasing the critical gradients beyond which microinstabilities are triggered, as was already suggested by past numerical simulation results [20].

Linear, flux-tube GENE simulations, run using the experimental profiles and equilibria of a pair of matched NB heated plasmas, found negative triangularity to have a stabilizing effect on the most unstable linear modes, especially for $k_y\rho_s < 1$, also in the presence of higher ion gradients and

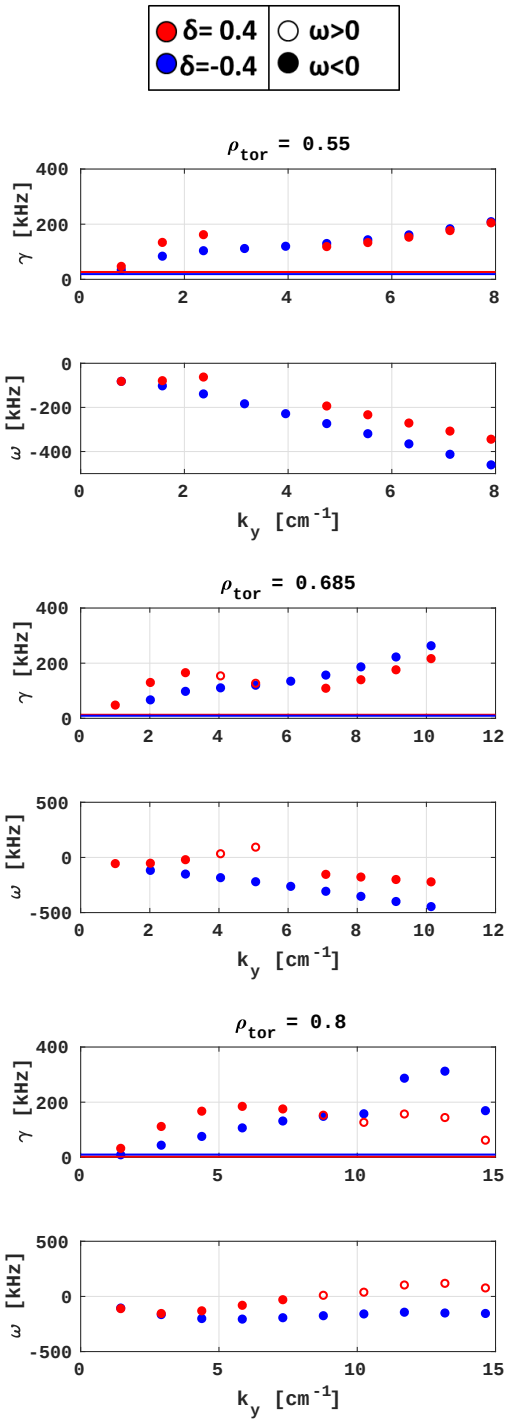

Figure 15: Results of the simulations for input equilibria and profiles corresponding to the ohmic plasmas. Linear growth rate (γ) and frequency (ω) of the most unstable mode for each wavenumber at three radial positions: $\rho_{tor} = 0.55$, $\rho_{tor} = 0.7$, $\rho_{tor} = 0.8$. Full markers correspond to modes that propagate in the electron diamagnetic direction (TEM or ETG). Quantities are presented in physical units, in the $0.2 < k_y\rho_s < 2$ range. The solid lines correspond to the estimated level of $E \times B$ shearing.

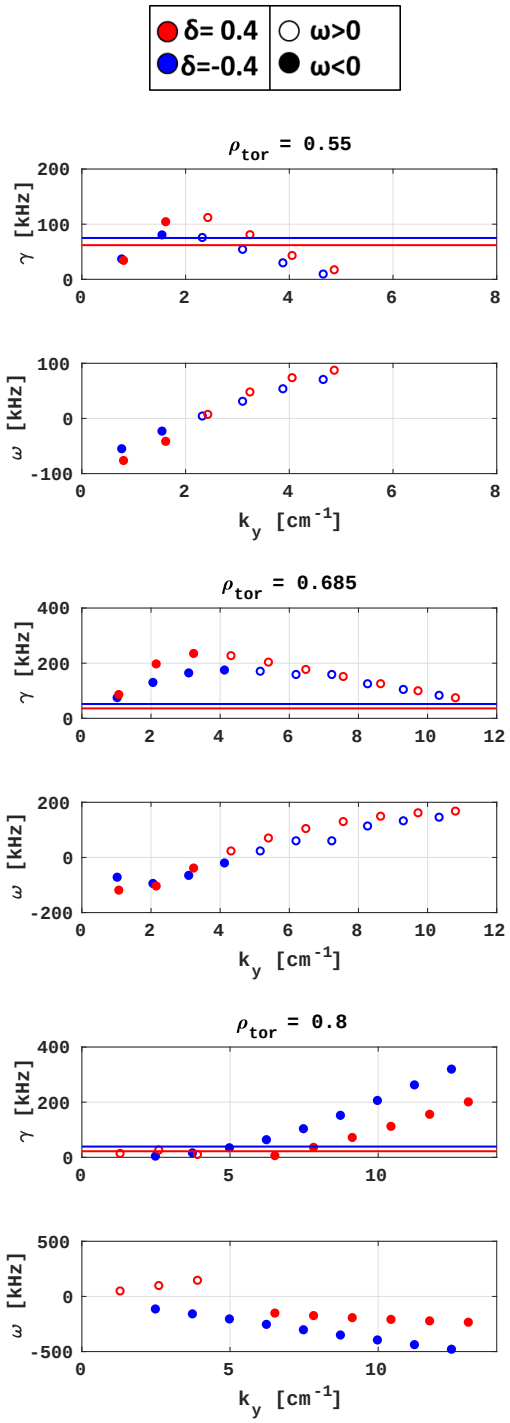

Figure 16: Results of the simulations for input equilibria and profiles corresponding to the NBI heated plasmas. Linear growth rate (γ) and frequency (ω) of the most unstable mode for each wavenumber in three radial positions: $\rho_{tor} = 0.55$, $\rho_{tor} = 0.65$, $\rho_{tor} = 0.8$. Full markers correspond to modes that propagate in the electron diamagnetic direction (TEM or ETG). Quantities are presented in physical units, in the $0.2 < k_y\rho_s < 2$ range. The solid lines correspond to the estimated level of $E \times B$ shearing for the two discharges.

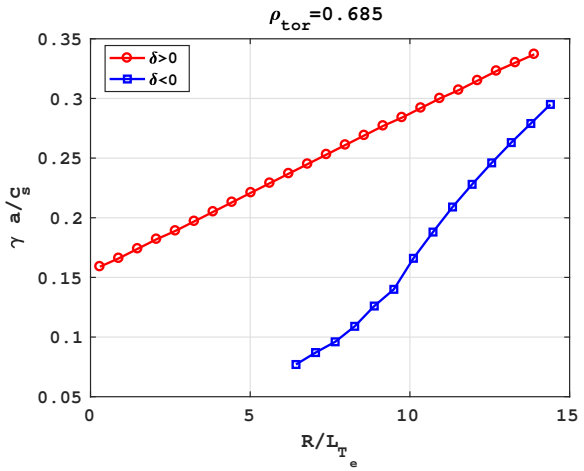

Figure 17: Normalized growth rates of the most unstable modes for $k_y\rho_s = 0.4$ with varying R/L_{Te} for parameters corresponding to NB heated plasmas. The critical gradient for exciting modes was found to be higher for negative δ.

$T_e/T_i < 1$. The observed differences in ω_{ExB} between positive and negative triangularity plasmas are too small with respect to the uncertainty related to their estimation to draw any reliable conclusion on a direct effect of negative triangularity. Linear simulations also supported the existence of an increased critical gradient for the onset of fluctuations in negative triangularity plasmas.

All together, these experiments and simulations point towards negative triangularity having a beneficial effect on confinement also in situations where ion driven turbulence becomes relevant, and thus closer to the operating space of future reactor-like machines.

The results found in this work are consistent with those found in DIII-D where a strong improvement in confinement was also observed for limited negative δ plasmas, subject to electron and ion heating. Also in that case, confinement was found to largely exceed the expectations for L-mode discharges, reaching up to levels comparable with positive δ H-mode plasmas.

More work is necessary to fully understand the effects of negative triangularity on fluctuations and the potential for a reactor-like negative δ tokamak. In this work, the effect of negative triangularity on plasma rotation could not be decoupled from that of ion heating. With the next upgrade phases planned in TCV, a second NBI will be installed, facing in the opposite direction as the one currently available. This setup will be used in the future to probe separately the effects of rotation and ion heating as was done on DIII-D [53] and Alcator C-mod [54]. The possibility of controlling the variation of toroidal momentum injected by the beam could also allow further understanding of the effects of shaping on ω_{ExB}.

A series of non-linear gyrokinetic simulations should be used to study the saturated turbulence in the mixed turbulence regime as was done for the pure TEM cases [19]. Furthermore, global simulations may be necessary to clarify the impact of non-local effects on the final heat transport profile [21]. The results of these simulations could be processed with a synthetic diagnostic for the CECE diagnostic [55] and compared with the experimental measurements.

Finally, to further approach the working conditions of future reactors, new experiments are forseen to test diverted configurations, with strike points residing both on the HFS and LFS.

Acknowledgements

The authors would like to thank A. Merle, A. Karpushov, F. Bagnato and A. Mariani for the very useful conversations and insights. This work has been carried out within the framework of the EUROfusion Consortium and has received funding from the Euratom research and training programme 2014-2018 and 2019-2020 under grant agreement No 633053. The views and opinions expressed herein do not necessarily reflect those of the European Commission This work was also performed partly in the framework of the Helmholtz Virtual Institute on Plasma Dynamical Processes and Turbulence Studies using Advanced Microwave Diagnostics. This work was supported in part by the Swiss National Science Foundation.

6. Bibliography

[1] A. J. Wootton, B. A. Carreras, H. Matsumoto, K. McGuire, W. A. Peebles, Ch. P. Ritz, P. W. Terry, and S. J. Zweben. Fluctuations and anomalous transport in tokamaks. *Physics of Fluids B: Plasma Physics*, 2(12):2879–2903, 1990.

[2] S. Coda and The TCV team. Overview of the TCV tokamak program: scientific progress and facility upgrades. *Nucl. Fusion*, 57(10):102011, 2017.

[3] J.-M. Moret, S. Franke, H. Weisen, M. Anton, R. Behn, B. P. Duval, F. Hofmann, B. Joye, Y. Martin, C. Nieswand, Z. A. Pietrzyk, and W. van Toledo. Influence of Plasma Shape on Transport in the TCV Tokamak. *Phys. Rev. Lett.*, 79(11):2057–2060, September 1997.

[4] A. Pochelon, T. P. Goodman, M. Henderson, C. Angioni, R. Behn, S. Coda, F. Hofmann, J.-P. Hogge, N. Kirneva, A. A. Martynov, J.-M. Moret, Z. A. Pietrzyk, F. Porcelli, H. Reimerdes, J. Rommers, E. Rossi, O. Sauter, M. Q. Tran, H. Weisen, S. Alberti, S. Barry, P. Blanchard, P. Bosshard, R. Chavan, B. P. Duval, Y.V. Esipchuck, D. Fasel, A. Favre, S. Franke, I. Furno, P. Gorgerat, P.-F. Isoz, B. Joye, J. B. Lister, X. Llobet, J.-C. Magnin, P. Mandrin, A. Manini, B. Marlétaz, P. Marmillod, Y. Martin, J.-M. Mayor, J. Mlynar, C. Nieswand, P. J. Paris, A. Perez, R. A. Pitts, K. A. Razumova, A. Refke, E. Scavino, A. Sushkov, G. Tonetti, F. Troyon, W. Van

Toledo, and P. Vyas. Energy confinement and MHD activity in shaped TCV plasmas with localized electron cyclotron heating. *Nucl. Fusion*, 39(11Y):1807, 1999.

[5] Y. Camenen, A. Pochelon, A. Bottino, S. Coda, F. Ryter, O. Sauter, R. Behn, T. P. Goodman, M. A. Henderson, A Karpushov, L. Porte, and G. Zhuang. Electron heat transport in shaped TCV L-mode plasmas. *Plasma Phys. Control. Fusion*, 47(11):1971, 2005.

[6] Y. Camenen, A. Pochelon, R. Behn, A. Bottino, A. Bortolon, S. Coda, A. Karpushov, O. Sauter, G. Zhuang, and the TCV team. Impact of plasma triangularity and collisionality on electron heat transport in TCV L-mode plasmas. *Nucl. Fusion*, 47(7):510, 2007.

[7] A. Pochelon, P. Angelino, R. Behn, S. Brunner, S. Coda, N. Kirneva, S. Yu Medvedev, H. Reimerdes, J. Rossel, O. Sauter, L. Villard, D. Wagner, A. Bottino, Y. Camenen, G. P. Canal, P. K. Chattopadhyay, B. P. Duval, A. Fasoli, T. P. Goodman, S. Jolliet, A. Karpushov, B. Labit, A. Marinoni, J.-M. Moret, A. PItzschke, L. Porte, M. Rancic, V. S. Udintsev, and the TCV Team. Recent TCV Results - Innovative Plasma Shaping to Improve Plasma Properties and Insight. *Plasma and Fusion Research*, 7:2502148–2502148, 2012.

[8] A. Marinoni, S. Coda, R. Chavan, and G. Pochon. Design of a tangential phase contrast imaging diagnostic for the TCV tokamak. *Review of Scientific Instruments*, 77(10):10E929, October 2006.

[9] Z. Huang and S. Coda. Dependence of density fluctuations on shape and collisionality in positive- and negative-triangularity tokamak plasmas. *Plasma Phys. Control. Fusion*, 61(1):014021, November 2018.

[10] Z. Huang. *Experimental study of plasma turbulence in the TCV tokamak*. PhD thesis, EPFL, 2017.

[11] L. Porte, S. Coda, C. A de Mejere, Z. Huang, P. Hennequin, A. Kramer-Flecken, L. Vermare, V. Vuille, S. Brunner, J. Dominsky, F. Margairaz, G. Merlo, T. Vernay, and L. Villard. Multi-Diagnostic Study of Core Turbulence and Geodesic Acoustic Modes in the TCV Tokamak. *Proceedings of the 25th IAEA FEC*, October 2014.

[12] M. Fontana, L. Porte, and P. Molina Cabrera. Correlation electron cyclotron emission diagnostic in TCV. *Review of Scientific Instruments*, 88(8):083506, 2017.

[13] M. Fontana, L. Porte, S. Coda, O. Sauter, and The TCV Team. The effect of triangularity on fluctuations in a tokamak plasma. *Nucl. Fusion*, 58(2):024002, 2018.

[14] A. Bottino, A. G. Peeters, O. Sauter, J. Vaclavik, and L. Villard. Simulations of global electrostatic microinstabilities in ASDEX Upgrade discharges. *Physics of Plasmas*, 11(1):198–206, 2003.

[15] M. Kotschenreuther, G. Rewoldt, and W. M. Tang. Comparison of initial value and eigenvalue codes for kinetic toroidal plasma instabilities. *Computer Physics Communications*, 88(2):128–140, 1995.

[16] F. Jenko, W. Dorland, M. Kotschenreuther, and B. N. Rogers. Electron temperature gradient driven turbulence. *Physics of Plasmas*, 7(5):1904–1910, 2000.

[17] T. Görler, X. Lapillonne, S. Brunner, T. Dannert, F. Jenko, F. Merz, and D. Told. The global version of the gyrokinetic turbulence code GENE. *Journal of Computational Physics*, 230(18):7053–7071, August 2011.

[18] F. Ryter, C. Angioni, A. G. Peeters, F. Leuterer, H.-U. Fahrbach, W. Suttrop, and ASDEX Upgrade Team. Experimental Study of Trapped-Electron-Mode Properties in Tokamaks: Threshold and Stabilization by Collisions. *Phys. Rev. Lett.*, 95(8):085001, August 2005.

[19] A. Marinoni, S. Brunner, Y. Camenen, S. Coda, J. P. Graves, X. Lapillonne, A. Pochelon, O. Sauter, and L. Villard. The effect of plasma triangularity on turbulent transport: modeling TCV experiments by linear and non-linear gyrokinetic simulations. *Plasma Phys. Control. Fusion*, 51(5):055016, 2009.

[20] G. Merlo, S. Brunner, O. Sauter, Y. Camenen, T. Görler, F. Jenko, A. Marinoni, D. Told, and L. Villard. Investigating profile stiffness and critical gradients in shaped TCV discharges using local gyrokinetic simulations of turbulent transport. *Plasma Phys. Control. Fusion*, 57(5):054010, 2015.

[21] Gabriele Merlo. *Flux-tube and global grid-based gyrokinetic simulations of plasma microturbulence and comparisons with experimental TCV measurements*. PhD thesis, EPFL, 2016.

[22] M. Kikuchi, T. Takizuka, and M. Furukawa. Negative Triangularity as a Possible Tokamak Scenario. In *Proceedings of the 12th Asia Pacific Physics Conference (APPC12)*, volume 1 of *JPS Conference Proceedings*. Journal of the Physical Society of Japan, March 2014.

[23] M. Kikuchi, S. Medvedev, T. Takizuka, A. Fasoli, Y. Wu, P. Diamond, X. Duan, Y. Kishimoto, K. Hanada, L. Villard, O. Sauter, S. Coda, B. Duval, H. Reimerdes, S. Brunner, G. Merlo, J. Jiang, M. Wang, M. Ni, D. Chen, H. Du, W. Duan, Y. Hou, A. Ivanov, A. Martynov, Y. Poshekhonov, Y. Ueda, L. Yan, X. Song, G. Zheng, J. Liu, K. Nagasaki, K. Imadera, K. Mishra, A. Fujisawa, K. Nakamura, H. Zushi, Mj Pueschel, X. Xu, P. Zhu, D. Told, G. Q. Li, M. Furukawa, T. Ozeki, K. Shimizu, K. Kawashima, H. Urano, M. Honda, T. Ando, and M. Kuriyama. Perspective of negative triangularity tokamak as fusion energy system. European Physical Society (EPS), January 2015.

[24] S. Yu Medvedev, M. Kikuchi, L. Villard, T. Takizuka, P. Diamond, H. Zushi, K. Nagasaki, X. Duan, Y. Wu, A.A. Ivanov, A. A. Martynov, Yu Yu Poshekhonov, A. Fasoli, and O. Sauter. The negative triangularity tokamak: stability limits and prospects as a fusion energy system. *Nucl. Fusion*, 55(6):063013, 2015.

[25] M. Kikuchi, T. Takizuka, S. Medvedev, T. Ando, D. Chen, J. X. Li, M. Austin, O. Sauter, L. Villard, A. Merle, M. Fontana, Y. Kishimoto, and K. Imadera. L-mode-edge negative triangularity tokamak reactor. *Nucl. Fusion*, 59(5):056017, April 2019.

[26] R. A. Pitts, S. Carpentier, F. Escourbiac, T. Hirai, V. Komarov, S. Lisgo, A. S. Kukushkin, A. Loarte, M. Merola, A. Sashala Naik, R. Mitteau, M. Sugihara, B. Bazylev, and P. C. Stangeby. A full tungsten divertor for ITER: Physics issues and design status. *Journal of Nuclear Materials*, 438:S48–S56, 2013.

[27] A. Loarte, B. Lipschultz, A. S. Kukushkin, G. F. Matthews, P. C. Stangeby, N. Asakura, G. F. Counsell, G. Federici, A. Kallenbach, K. Krieger, A. Mahdavi, V. Philipps, D. Reiter, J. Roth, J. Strachan, D. Whyte, R. Doerner, T. Eich, W. Fundamenski, A. Herrmann, M. Fenstermacher, P. Ghendrih, M. Groth, A. Kirschner, S. Konoshima, B. LaBombard, P. Lang, A. W. Leonard, P. Monier-Garbet, R. Neu, H. Pacher, B. Pegourie, R.A. Pitts, S. Takamura, J. Terry, E. Tsitrone, the ITPA Scrape-off Layer, and Divertor Physics Topical Group. Chapter 4: Power and particle control. *Nucl. Fusion*, 47(6):S203, 2007.

[28] M. Faitsch, R. Maurizio, A. Gallo, S. Coda, T. Eich, B. Labit, A. Merle, H. Reimerdes, B. Sieglin, C. Theiler, the Eurofusion MST1 Team, and the TCV Team. Dependence of the L-Mode scrape-off layer power fall-off length on the upper triangularity in TCV. *Plasma Phys. Control. Fusion*, 60(4):045010, 2018.

[29] M. E. Austin, A. Marinoni, M. L. Walker, M. W. Brookman, J. S. deGrassie, A. W. Hyatt, G. R. McKee, C. C. Petty, T. L. Rhodes, S. P. Smith, C. Sung, K. E. Thome, and A. D. Turnbull. Achievement of Reactor-Relevant

Performance in Negative Triangularity Shape in the DIII-D Tokamak. *Phys. Rev. Lett.*, 122(11):115001, March 2019.

[30] A. Marinoni, M. E. Austin, A. W. Hyatt, M. L. Walker, J. Candy, C. Chrystal, C. J. Lasnier, G. R. McKee, T. Odstrčil, C. C. Petty, M. Porkolab, J. C. Rost, O. Sauter, S. P. Smith, G. M. Staebler, C. Sung, K. E. Thome, A. D. Turnbull, and L. Zeng. H-mode grade confinement in L-mode edge plasmas at negative triangularity on DIII-D. *Physics of Plasmas*, DPP60(1):042515, April 2019.

[31] A. N. Karpushov, R. Chavan, S. Coda, V. I. Davydenko, Frédéric Dolizy, A. N. Dranitchnikov, B. P. Duval, A. A. Ivanov, D. Fasel, A. Fasoli, V. V. Kolmogorov, P. Lavanchy, X. Llobet, B. Marlétaz, P. Marmillod, Y. Martin, A. Merle, A. Perez, O. Sauter, U. Siravo, I. V. Shikhovtsev, A. V. Sorokin, and M. Toussaint. Neutral beam heating on the TCV tokamak. *Fusion Engineering and Design*, 123:468–472, November 2017.

[32] G. V. Pereverzev and P. N. Yushmanov. ASTRA - Automated System for TRansport Analysis. Technical Report IPP report, Max-Planck-Institut Für Plasmaphysik, 2002.

[33] E. Fable, C. Angioni, F. J. Casson, D. Told, A. A. Ivanov, F. Jenko, R. M. McDermott, S. Yu Medvedev, G. V. Pereverzev, F. Ryter, W. Treutterer, and E. Viezzer and. Novel free-boundary equilibrium and transport solver with theory-based models and its validation against ASDEX Upgrade current ramp scenarios. *Plasma Phys. Control. Fusion*, 55(12):124028, November 2013.

[34] A. Polevoi, H. Shirai, and T. Takizuka. Benchmarking of the NBI block in ASTRA code versus the OFMC calculations. Technical Report JAERI-DATA/CODE–97-014, Japan Atomic Energy Research Inst., 1997.

[35] B. Geiger, A. N. Karpushov, B. P. Duval, C. Marini, O. Sauter, Y. Andrebe, D. Testa, M. Marascheck, M. Salewski, P. A. Schneider, and and. Fast-ion transport in low density L-mode plasmas at TCV using FIDA spectroscopy and the TRANSP code. *Plasma Phys. Control. Fusion*, 59(11):115002, September 2017.

[36] Matteo Fontana. *Turbulence studies in TCV using the Correlation ECE diagnostic*. PhD thesis, EPFL, 2018.

[37] C. Angioni, T. P. Goodman, M. A. Henderson, and O. Sauter. Effects of localized electron heating and current drive on the sawtooth period. *Nucl. Fusion*, 43(6):455–468, May 2003.

[38] T. D. Rempel, R. F. Gandy, and A. J. Wootton. Density fluctuation effects on electron cyclotron emission correlation measurements in optically gray plasmas. *Review of Scientific Instruments*, 65(6):2044–2048, 1994.

[39] C. Angioni, E. Fable, M. Greenwald, M. Maslov, A. G. Peeters, H. Takenaga, and H. Weisen. Particle transport in tokamak plasmas, theory and experiment. *Plasma Phys. Control. Fusion*, 51(12):124017, November 2009.

[40] J. Hawke, Y. Andrebe, R. Bertizzolo, P. Blanchard, R. Chavan, J. Decker, B. Duval, P. Lavanchy, X. Llobet, B. Marlétaz, P. Marmillod, G. Pochon, and M. Toussaint. Improving spatial and spectral resolution of TCV Thomson scattering. *J. Inst.*, 12(12):C12005, 2017.

[41] O. Sauter, C. Angioni, and Y. R. Lin-Liu. Neoclassical conductivity and bootstrap current formulas for general axisymmetric equilibria and arbitrary collisionality regime. *Physics of Plasmas*, 6(7):2834–2839, 1999.

[42] O. Sauter, C. Angioni, and Y. R. Lin-Liu. Erratum: "Neoclassical conductivity and bootstrap current formulas for general axisymmetric equilibria and arbitrary collisionality regime" [Phys. Plasmas 6, 2834 (1999)]. *Physics of Plasmas*, 9(12):5140–5140, November 2002.

[43] J. C. Hillesheim, J. C. DeBoo, W. A. Peebles, T. A. Carter, G. Wang, T. L. Rhodes, L. Schmitz, G. R. McKee, Z. Yan, G. M. Staebler, K. H. Burrell, E. J. Doyle, C. Holland, C. C. Petty, S. P. Smith, A. E. White, and L. Zeng. Observation of a Critical Gradient Threshold for Electron Temperature Fluctuations in the DIII-D Tokamak. *Phys. Rev. Lett.*, 110(4):045003, January 2013.

[44] O. Sauter, S. Brunner, D. Kim, G. Merlo, R. Behn, Y. Camenen, S. Coda, B. P. Duval, L. Federspiel, T. P. Goodman, A. Karpushov, A. Merle, and Tcv Team. On the non-stiffness of edge transport in L-mode tokamak plasmas. *Physics of Plasmas*, 21(5):055906, 2014.

[45] ITER Physics Expert Group on Confinement, Transport, ITER Physics Expert Group on Confinement Modelling, Database, and ITER Physics Basis Editors. Chapter 2: Plasma confinement and transport. *Nucl. Fusion*, 39(12):2175, 1999.

[46] P. N. Yushmanov, T. Takizuka, K. S. Riedel, O. J. W. F. Kardaun, J. G. Cordey, S. M. Kaye, and D. E. Post. Scalings for tokamak energy confinement. *Nucl. Fusion*, 30(10):1999–2006, October 1990.

[47] T. S. Hahm. Rotation shear induced fluctuation decorrelation in a toroidal plasma. *Physics of Plasmas*, 1(9):2940–2944, September 1994.

[48] T. S. Hahm and K. H. Burrell. Role of flow shear in enhanced core confinement regimes. *Plasma Phys. Control. Fusion*, 38(8):1427–1431, August 1996.

[49] T. Casper, Y. Gribov, A. Kavin, V. Lukash, R. Khayrutdinov, H. Fujieda, C. Kessel, and and. Development of the ITER baseline inductive scenario. *Nucl. Fusion*, 54(1):013005, December 2013.

[50] Claudio Marini. *Poloidal CX visible light plasma rotation diagnostics in TCV*. PhD thesis, EPFL, 2017.

[51] G. Merlo, M. Fontana, S. Coda, D. Hatch, S. Janhunen, L. Porte, and F. Jenko. Turbulent transport in TCV plasmas with positive and negative triangularity. *Physics of Plasmas*, 26(10):102302, October 2019.

[52] P. W. Terry. Suppression of turbulence and transport by sheared flow. *Rev. Mod. Phys.*, 72(1):109–165, January 2000.

[53] L. Schmitz, A. E. White, T. A. Carter, W. A. Peebles, T. L. Rhodes, K. H. Burrell, W. Solomon, and G. M. Staebler. Observation of Reduced Electron-Temperature Fluctuations in the Coreof H-Mode Plasmas. *Phys. Rev. Lett.*, 100(3):035002, January 2008.

[54] A. E. White, M. Barnes, A. Dominguez, M. Greenwald, N. T. Howard, A. E. Hubbard, J. W. Hughes, D.R. Mikkelsen, F. I. Parra, M. L. Reinke, C. Sung, J. Walk, and D. G. Whyte. Reduction of core turbulence in I-mode plasmas in Alcator C-Mod. *Nucl. Fusion*, 54(8):083019, 2014.

[55] A.e. White, W.a. Peebles, T.l. Rhodes, G. Wang, L. Schmitz, T.a. Carter, J.c. Hillesheim, E.j. Doyle, L. Zeng, C.h. Holland, G.r. Mckee, G.m. Staebler, R.e. Waltz, J. Candy, J.c. DeBOO, C.c. Petty, and K.h. Burrell. Correlation ece measurements of turbulent electron temperature fluctuations in diii-d. In *Electron Cyclotron Emission and Electron Cyclotron Resonance Heating (EC-16)*, pages 168–173. WORLD SCIENTIFIC, February 2011.